Thermochimica Acta 556 (2013) 41–46

Contents lists available at SciVerse ScienceDirect

Thermochimica Acta

journal homepage: www.elsevier.com/locate/tca

Synthesis, thermo-analytical and IR spectral studies of hydrazinated mixed metal carboxylates: A single source precursor to nanosize mixed metal oxides

U.B. Gawas, V.M.S. Verenkar*

Department of Chemistry, Goa University, Taleigao Plateau, Goa 403 206, India

ARTICLE INFO

Article history:
Received 7 December 2012
Received in revised form 17 January 2013
Accepted 20 January 2013
Available online 8 February 2013

Keywords:
Thermal decomposition
Hydrazinated metal fumarates
Nanoparticles
Ferrites

ABSTRACT

A series of hydrazinated mixed nickel manganese zinc ferrous hydrazine fumarate complexes were synthesized from aqueous mixed metal chloride solutions and sodium fumarate-hydrazine hydrate mixture. The detailed characterization was carried out by chemical analysis, infrared spectroscopy and isothermal mass loss studies. The hydrazine ligand in these complexes shows bidentate bridging nature while fumarate anion exhibit monodentate behavior. These complexes act as single source precursors for nanosize ferrites. Thermal decomposition of these precursors was studied upto 800 °C in static air using simultaneous TG/DTA. The thermal decomposition study indicates 3-step decomposition of these precursors into nanosize mixed metal oxides. The nanosize mixed metal oxides were then characterized by X-ray diffraction, transmission electron microscopy and infrared spectral studies.

1. Introduction

Spinel ferrites are ceramic materials widely investigated because of their interesting electrical and magnetic properties which are useful in applications such as information storage systems, magnetic bulk cores, magnetic fluids, microwave absorbers, medical diagnostics etc. [1,2]. The most recent reason for the upsurge in interest in ferrite is because of development of the new, small, efficient power supplies using solid state switching called switch mode power supplies (SMPs). These SMP's are the integral components of modern day electronic equipments such as computers, laptops and entertainment applications [3]. Besides the ease of preparation and low manufacturing cost, the advantage of spinel ferrites is their high magnetic permeability and high electrical resistivity. Also these materials can be shaped in a variety of different geometries meant for specific applications. Due to their applications, the ferrites have been prepared by several wet chemical techniques [4–9] and one of the important among them is precursor technique [10,11]. Several metal as well mixed metal carboxylates (mono and di) has been investigated in detail for structure, thermal decomposition [12] and their application as a precursor for synthesis of industrially important ferrites [13]. Recently, the focus has been shifted on the use of hydrazinated metal carboxylates to yield metal oxides at relatively lower temperatures. Although, commercially hydrazine is used as a monopropellant and rocket fuel, it can also serve as very good ligand because of the lone pairs present on nitrogen atoms and hence neutral hydrazine can coordinate to the metal ions as either monodentate ligand or bridging bidentate ligand to form complexes. Neutral hydrazine complexes are thermally more reactive than mono protonated hydrazine or hydrazinium complexes. Hence, the complexes containing neutral hydrazine molecules such as hydrazinated metal carboxylates are gaining importance, as they can act as a single source precursor to prepare stiochiometrically pure and nanosize mixed metal oxides [14] at relatively lower temperatures and shorter time. Several researchers have employed these hydrazinated complexes of metal as well as mixed metal carboxylates (mono and di) for the synthesis of oxide materials such as γ-Fe_2O_3 [15], ferrites [16,17], manganites [18,19], cobaltites [14,20], perovskites [21], ceramic abrasives like titania, zirconia [22] etc. which are technologically important. Many hydrazinated metal carboxylates such as metal formate [23], acetate [24] and dicarboxylates like oxalate [17,25,26], malonates, succinates [14,18–20,27–29], maleate [30], malate [31] and fumarate [32–44] have been used for the synthesis of metal oxides as well as mixed metal oxides of technological importance. The present study reports synthesis, characterization, thermal and infrared spectral studies of hydrazinated mixed nickel manganese zinc ferrous fumarate complexes (which acts as a precursors) and their decomposed end products.

2. Experimental

2.1. Preparation

The synthesis of hydrazinated mixed nickel manganese zinc ferrous hydrazine fumarate complexes were carried out by adding

* Corresponding author. Tel.: +91 832 6519321; fax: +91 832 2452886.
E-mail address: vmsv@rediffmail.com (V.M.S. Verenkar).

0040-6031/$ – see front matter © 2013 Elsevier B.V. All rights reserved.
http://dx.doi.org/10.1016/j.tca.2013.01.017

aqueous metal chloride solutions to sodium fumarate-hydrazine hydrate mixture stirred in N_2 atmosphere. The yellow colored precipitates of complexes obtained were filtered, washed with ethanol and dried with diethyl ether on suction. The formations of these complexes occurs by the following reaction

$$MCl_{2(aq)} + 2FeCl_{2(aq)} + 3Na_2C_4H_2O_{4(aq)} + 6N_2H_4.H_2O_{(aq)} \rightarrow MFe_2(C_4H_2O_4)_3{\cdot}6N_2H_{4(s)} + 6NaCl_{(aq)} + 6H_2O_{(l)}$$

$(M = Ni^{2+}, Mn^{2+}, Zn^{2+})$

2.2. Characterization

The molecular compositions of the synthesized precursors were determined by standard procedures of chemical analysis. The hydrazine analyses of the precursors were carried out by using standard 0.025 M KIO_3 solution as a titrant under Andrew's conditions [45]. The metal contents in precursors were determined by chemical analysis after decomposing the known amount of precursors with concentrated nitric acid using standard procedures. The iron and nickel contents were determined gravimetrically as Fe_2O_3 and nickel-dimethylglyoximato complex respectively, while manganese and zinc were determined together complexometrically using suitable masking agent [45]. The simultaneous thermogravimetric (TG) and differential thermal analysis (DTA) of the precursors as well as decomposed end products were carried out in air at a heating rate of 10 deg-min^{-1} using NETZSCH DSC-DTA-TG STA 409PC Luxx thermal analyser. Alumina cups were used for holding the 10–15 mg sample for the analyses. The isothermal and total mass loss studies of the precursors were done along with hydrazine estimation at various predetermined temperatures. The infrared spectra of the precursors and decomposed end products were recorded on FTIR Shimadzu IR prestige21 series spectrophotometer. The decomposed end products were analyzed for structure and phase purity by Philips X-ray diffractometer model PW 1710 with CuK_α radiations and Ni filter. The TEM micrographs were taken using Philip's-CM20 electron microscope.

2.3. Thermolysis of the hydrazinated mixed metal fumarates

The thermal decomposition of precursor complexes in air occurs by following reaction:

$$6MFe_2(C_4H_2O_4)_3{\cdot}6N_2H_{4(s)} + 35O_{2(g)} \rightarrow 6MFe_2O_{4(s)} + 24CO_{2(g)} + 12N_{2(g)} + 72H_2O_{(g)}$$

$(M = Mn^{2+}, Ni^{2+}, Zn^{2+})$

The thermal decomposition of precursors was found to be self propagating and autocatalytic. For self propagating autocatalytic decomposition, the precursors were spread uniformly over a ceramic tile and ignited with a burning splinter at one of the end. The precursors catch fire and burn without flame forming a red glow which spreads over the entire bulk completing the total decomposition in an ordinary atmosphere, within few minutes. During thermal decomposition of precursor in air, small atomic clusters of nascent metal oxides with proper chemical homogeneity are formed. These clusters react together and forms nanosize ferrites. The heat required for the formation of nanosize ferrites was provided by the combustion of hydrazine and carbonaceous mass of fumarate precursor. Also, the evolution of various gases like water vapour, CO_2 and N_2 during oxidative decomposition of the precursor helps in the dissipation of the heat of decomposition, thereby preventing the sintering of nanosize ferrite particles soon after their formation [46,47].

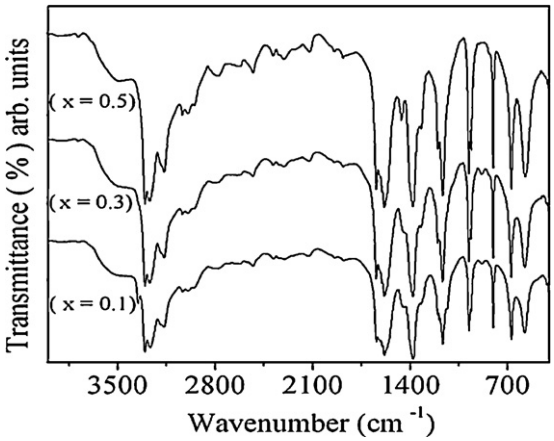

Fig. 1. FTIR spectrum of $Ni_{0.5-x}Mn_xZn_{0.5}Fe_2(C_4H_2O_4)_3{\cdot}6N_2H_4$ (x = 0.1,0.3,0.5).

3. Results and discussion

3.1. Chemical analysis and IR spectral studies

The thermo-analytical data of the precursors obtained by chemical and thermal analysis was used to fix the formulae of the precursors. Based on the chemical analysis (Table 1) and total mass loss studies (Table 2), the molecular stoichiometric compositions were assigned to the hydrazinated mixed nickel manganese zinc ferrous fumarate precursors. The observed percentages matches closely with calculated percentages of metals, hydrazine and total mass losses of the precursors (Tables 1 and 2) suggesting the formulae given in Table 1. Some representative FTIR spectra are shown in Fig. 1. The infrared (IR) spectra of precursors were recorded from 4000 cm^{-1} to 400 cm^{-1}. The IR peaks characteristics of N—H stretching vibrations of hydrazine in the precursors were observed in the region 3355–3167 cm^{-1}, while peak due NH_2 deformation was observed in the range 1585–1581 cm^{-1} (Table 3). The N—N stretching frequencies observed at 980 cm^{-1} were found to be characteristics of bidentate bridge linkage of hydrazine ligands in

Table 1
Chemical analysis results of hydrazine complexes of mixed nickel manganese zinc ferrous fumarates, $Ni_{0.5-x}Mn_xZn_{0.5}Fe_2(C_4H_2O_4)_3.6N_2H_4$ (x = 0.0–0.5).

Complex comp. (x)	Metal content (%)								Hydrazine (%)		Proposed molecular formula	Molecular mass
	Fe		Mn		Ni		Zn					
	Obs.	Calc.	Obs.	Calc.	Obs.	Calc.	Obs.	Calc.	Obs.	Calc.		
0.0	15.75	15.77	–		4.11	4.15	4.59	4.61	27.12	27.16	$Ni_{0.5}Zn_{0.5}Fe_2(C_4H_2O_4)_3.6N_2H_4$	708.2
0.1	15.77	15.78	0.76	0.77	3.30	3.32	4.58	4.62	27.29	27.17	$Ni_{0.4}Mn_{0.1}Zn_{0.5}Fe_2(C_4H_2O_4)_3.6N_2H_4$	707.8
0.2	15.80	15.79	1.51	1.56	2.48	2.49	4.60	4.62	27.39	27.18	$Ni_{0.3}Mn_{0.2}Zn_{0.5}Fe_2(C_4H_2O_4)_3.6N_2H_4$	707.4
0.3	15.81	15.80	2.30	2.33	1.63	1.66	4.57	4.62	27.24	27.20	$Ni_{0.2}Mn_{0.3}Zn_{0.5}Fe_2(C_4H_2O_4)_3.6N_2H_4$	707.1
0.4	15.83	15.81	3.08	3.11	0.826	0.832	4.61	4.62	27.49	27.21	$Ni_{0.1}Mn_{0.4}Zn_{0.5}Fe_2(C_4H_2O_4)_3.6N_2H_4$	706.7
0.5	15.80	15.82	3.86	3.89	–		4.55	4.63	27.16	27.22	$Mn_{0.5}Zn_{0.5}Fe_2(C_4H_2O_4)_3.6N_2H_4$	706.3

Table 2
Total mass loss and isothermal mass loss studies results of hydrazinated complexes of mixed nickel manganese zinc ferrous fumarates, $Ni_{0.5-x}Mn_xZn_{0.5}Fe_2(C_4H_2O_4)_3{\cdot}6N_2H_4$ (x = 0.0–0.5).

Compo. (x)	Total mass loss (%)		Isothermal mass loss studies (%), hydrazine content (%)			
	Pyrolysis in air (Obs.)	Calc.	RT-75 °C	75–100 °C	100–125 °C	125–150 °C
0.0	67.41	66.44	4.21/28.75	5.26/23.78	1.60/20.66	56.76/complex decomposed
0.1	66.99	66.47	4.44/28.21	5.53/23.40	1.65/23.76	53.51/complex decomposed
0.2	67.26	66.50	2.26/27.23	5.15/24.43	1.10/23.60	58.41/complex decomposed
0.3	67.53	66.54	3.56/28.13	4.67/22.70	1.51/21.56	54.93/complex decomposed
0.4	66.99	66.57	4.32/28.32	5.12/24.45	1.72/18.40	57.91/complex decomposed
0.5	67.15	66.68	2.44/27.85	4.63/22.46	1.53/20.54	56.75/complex decomposed

Table 3
FTIR absorption frequencies of $Ni_{0.5-x}Mn_xZn_{0.5}Fe_2(C_4H_2O_4)_3.6N_2H_4$ (x = 0.0–0.5) precursor complexes.

Compo. (x)	IR absorptions (cm^{-1})							
	N—H stretching	ν_{asym} COO^- stretching	NH_2 deformation	ν_{sym} COO^- stretching	NH_2 wagging	N—N stretching	N—N bending	NH_2 rocking
0.0	3355–3167	1644	1585	1380	1164	980	802	674
0.1	3355–3167	1644	1584	1380	1164	980	802	670
0.2	3304–3167	1644	1581	1380	1165	980	803	674
0.3	3304–3167	1644	1581	1380	1165	980	803	670
0.4	3304–3167	1644	1581	1380	1165	980	803	670
0.5	3304–3167	1644	1581	1380	1165	980	803	670

the complexes [48,49]. The asymmetric stretching vibration (ν_{asy}) frequencies of the fumarate ion in the precursors were observed at 1644 cm^{-1} while symmetric stretching vibration (ν_{sy}) frequencies appeared at 1380 cm^{-1}, with a separation $\Delta\nu$ ($\nu_{asy} - \nu_{sym}$) of 264 cm^{-1} confirming the monodentate linkage behavior of both carboxylate groups in the fumarate dianions [50]. Thus, the FTIR analysis points toward the bidentate bridging nature of neutral hydrazine ligands and monodentate linkage of fumarate dianions and hence, the polymeric nature of hydrazinated mixed nickel manganese zinc ferrous fumarate precursors.

3.2. TG and DTA analysis

The thermal analysis of hydrazinated mixed nickel manganese zinc ferrous fumarate precursors has been studied isothermally upto 150 °C and non-isothermally using TG/DTA upto 800 °C. The profiles of some of the synthesized precursors are represented in the Figs. 2–4, while the thermal decomposition data of all the precursors is tabulated in Table 4. The thermal decomposition of all the $Ni_{0.5-x}Mn_xZn_{0.5}Fe_2(C_4H_2O_4)_3{\cdot}6N_2H_4$ (x = 0.0–0.5) precursors occurs in three steps. The initial mass losses of 10.19%, 10.22%, 10.46% and 9.95% in precursors with composition, x = 0.0, 0.1, 0.3 and 0.4, respectively from RT −110 °C were due to the loss of adsorbed species including moisture (desorption) and beginning of the dehydrazination. This desorption of adsorbed species was indicated by a weak endotherm in the temperature range 80–90 °C, while the hydrazine loss was indicated by weak exotherm in the DTA curve in the region from 90 °C to 110 °C. The mass loss of 3.10% and 3.05% observed in precursors with composition, x = 0.2 and 0.5,

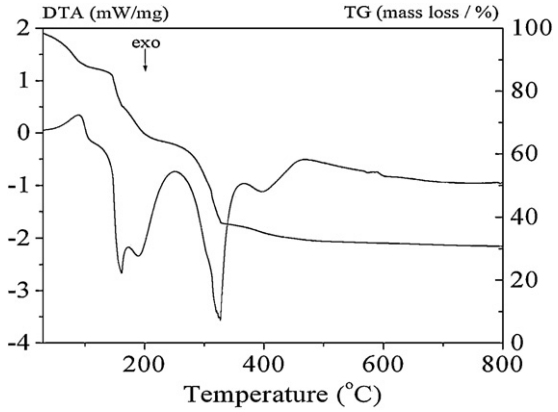

Fig. 3. TG/DTA profile $Ni_{0.3}Mn_{0.2}Zn_{0.5}Fe_2(C_4H_2O_4)_3{\cdot}6N_2H_4$ complex.

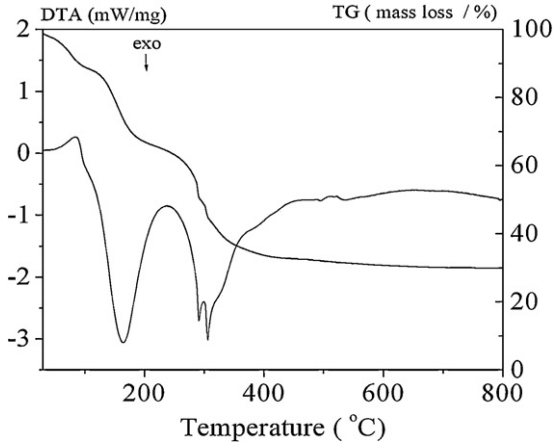

Fig. 2. TG/DTA profile of $Ni_{0.5}Zn_{0.5}Fe_2(C_4H_2O_4)_3{\cdot}6N_2H_4$ complex.

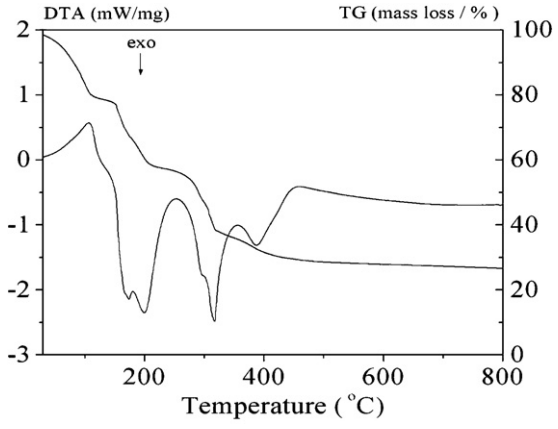

Fig. 4. TG/DTA profile of $Ni_{0.1}Mn_{0.4}Zn_{0.5}Fe_2(C_4H_2O_4)_3{\cdot}6N_2H_4$ complex.

Table 4
TG/DTA analysis data of hydrazinated mixed nickel manganese zinc ferrous fumarates, $Ni_{0.5x}Mn_xZn_{0.5}Fe_2(C_4H_2O_4)_3{\cdot}6N_2H_4$ (x = 0.0–0.5).

Compo. (x)	TG (mass loss (%))/DTA (mW mg^{-1}/°C)						
	RT-110	110–170	170–210	110–210	210–360	360–460	RT-460
0.0	10.19/84.4 (endo)	–	–	22.21/164.8 (exo)	29.85/292, 307 (exo)	3.58/∼386 (exo hump)	65.83
0.1	10.22/89.2 (endo)	17.86/153.8 (exo)	5.4/181.7 (exo)	–	28.33/306 (exo)	5.08/391.2 (exo)	66.89
0.2	3.10/89.8 (exo)	–	–	23.74/186.8 (exo)	33.68/327.3 (exo)	3.58/∼386 (exo hump)	65.36
0.3	10.46/89 (endo)	16.85/161.7 (exo)	5.6/188.9 (exo)	–	27.81/327.3 (exo)	5.62/396 (exo)	66.33
0.4	9.95/89.7 (endo)	17.79/156.9 (exo)	5.04/182.4 (exo)	–	28.84/300.6 (exo)	5.36/370.8 (exo)	66.98
0.5	3.05/98.6 (exo)	–	–	26.04/180.7 (exo)	30.13/293.4 (exo)	8.41/373.2 (exo)	67.63

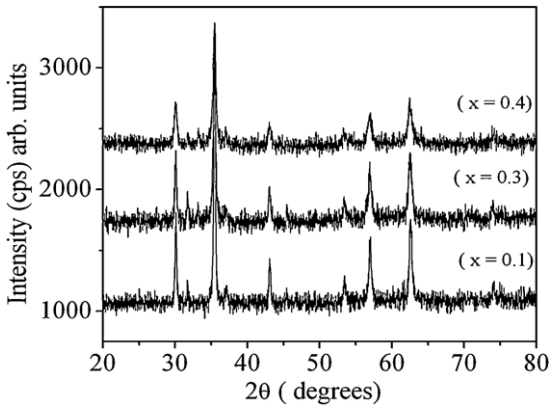

Fig. 5. XRD pattern of $Ni_{0.5-x}Mn_xZn_{0.5}Fe_2O_4$ (x = 0.1, 0.3, 0.4) ferrite.

respectively, indicates very low moisture contents. Infact, the DTA curve display only a weak exotherm which marks the beginning of dehydrazination from room temperature to 110 °C. The mass loss of 17.86%, 16.85% and 17.79% observed in precursors with composition, x = 0.1, 0.3 and 0.4, respectively in the region 110–170 °C corresponds to the loss of four hydrazine molecules. The DTA profile displays strong exotherm with peak temperature of 153.8 °C, 161.6 °C and 156.9 °C corresponding to this dehydrazination and, the mass loss of 5.4%, 5.6% and 5.04% observed from 170 °C to 210 °C was due to the complete dehydrazination of these complexes. The exothermic peaks in DTA were observed at 181.7 °C, 188.9 °C and 182.4 °C for composition, x = 0.1, 0.3 and 0.4 respectively. In the complexes with composition, x = 0.0, 0.2 and 0.5, this dehydrazination was found to occur in one step with mass losses of 22.21%, 23.74%, and 26.04%, respectively in the temperature region from 110 °C to 210 °C. The single step dehydrazination was indicated by strong exothermic peak at 164.8 °C, 186.8 °C and 180.7 °C, respectively in the DTA profiles. The mass loss region from 210 °C to 360 °C with mass losses from 27.81% to 33.68% results from the oxidative decarboxylation of dehydrazinated precursors with corresponding strong exotherms in DTA in this region. The high exothermicity of dehydrazination acts as a driving force for low temperature decarboxylation of dehydrazinated precursors. The marginal mass loss region (3.58–8.41% mass loss) with broad exotherm in DTA from 330 °C to 460 °C results from the oxidation of the residual carbon formed during decarboxylation. The total mass losses obtained from thermogravimetric measurement and those obtained from pyrolysis of complexes in air were found to be slightly higher than the calculated values considering the stoichiometric molecular composition assigned to the precursor complexes (Table 4). The difference observed was due to high concentration of adsorbed species like moisture on these precursor complexes. The presence of adsorbed moisture was also reflected in the FTIR spectra of complexes wherein weak band due to O–H stretching appears in the region 3550–3460 cm^{-1}. The initial increase in the hydrazine content observed upto 75 °C during isothermal mass loss studies also supports the above observations.

3.3. Isothermal moss loss and hydrazine analysis

The isothermal mass loss studies were carried out at various predetermined temperatures along with the hydrazine analysis

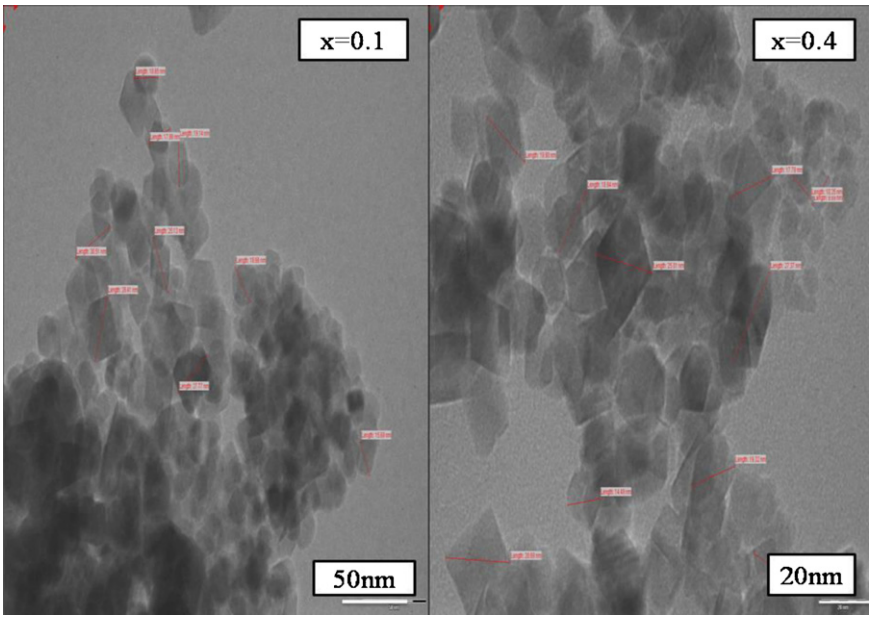

Fig. 6. TEM micrograph of $Ni_{0.5-x}Mn_xZn_{0.5}Fe_2O_4$ (x = 0.1, 0.4) ferrites.

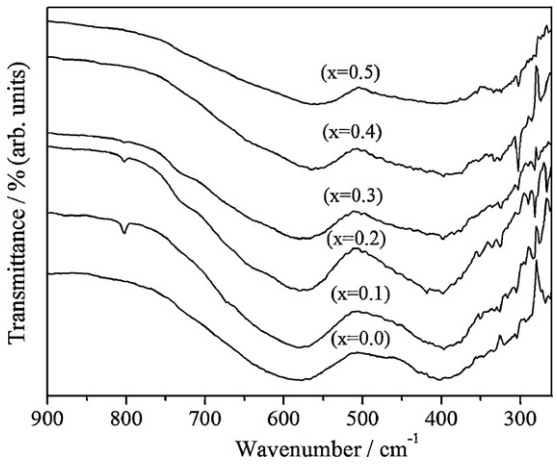

Fig. 7. FTIR spectra of $Ni_{0.5-x}Mn_xZn_{0.5}Fe_2O_4$ ($x = 0.0–0.5$) ferrites.

at every temperature in programmable electric oven. For complexes with composition, $x = 0.0$, 0.1, 0.3 and 0.4, the mass loss of 3.56–4.44% was observed from room temperature to75 °C, but hydrazine analysis showed increase in the hydrazine content which indicated the loss of volatile adsorbed species including moisture (Table 2), while for complexes with $x = 0.2$ and 0.5 the mass loss observed upto 75 °C was comparatively smaller which indicated low concentration of adsorbed species. When these precursors were heated to 100 °C, the mass loss observed corresponds to loss of about one hydrazine as can be seen from (Table 2) decrease in hydrazine content. On further heating these precursors upto temperature of 125 °C, a marginal mass loss was observed along with the decrease of hydrazine content indicating continuous dehydrazination, but when the temperature was slowly raised above 125 °C, the complexes were found to undergo combustion which was self propagating and autocatalytic.

3.4. Characterization of decomposed end products

The X-ray diffraction (XRD) patterns of the decomposed end products were recorded in the range of 20–80°. The end products were found to be monophasic as indicated by some representative X-ray diffraction pattern shown in Fig. 5. The XRD patterns display all the peaks characteristics of cubic spinel ferrites without any noticeable impurity peak indicating the formation of $Ni_{0.5-x}Mn_xZn_{0.5}Fe_2O_4$ ($x = 0.0–0.5$), while the broadening of XRD peaks indicates their nanocrystalline nature. The average crystallite size calculated from XRD peaks using Scherrer formula was found to be in the range 19–28 nm. The nanosize nature of $Ni_{0.5-x}Mn_xZn_{0.5}Fe_2O_4$ ($x = 0.0–0.5$) ferrite particles was also confirmed from the TEM studies. The particle size in the range 12–50 nm was observed in the TEM micrograph (Fig. 6). The FTIR spectra of the decomposed end products were recorded from 1000 cm^{-1} to 340 cm^{-1}. The IR band due to metal-oxygen stretching vibrations (ν_1) in tetrahedral sites of ferrites was observed (Fig. 7) in the region 582–560 cm^{-1} while the bands (ν_2) observed in the region 402–333 cm^{-1} represents metal-oxygen stretching vibrations in octahedral sites [51,52]. These FTIR spectral results supports the formation of $Ni_{0.5-x}Mn_xZn_{0.5}Fe_2O_4$ ($x = 0.0–0.5$) ferrites.

4. Conclusions

The synthetic route designed by our group was successfully employed for preparation of nanosize nickel manganese zinc ferrites. Following are the conclusions drawn from the present investigation.

1. The hydrazinated mixed nickel manganese zinc ferrous fumarate precursors were synthesized from sodium fumarate, metal chlorides and hydrazine hydrate at room temperature.
2. The chemical analysis, thermo-analytical and infrared spectral studies of the complexes confirms their formation with stoichiometric composition viz. $Ni_{0.5-x}Mn_xZn_{0.5}Fe_2(C_4H_2O_4)_3.6N_2H_4$ ($x = 0.0–0.5$).
3. The TG/DTA studies has showed different decomposition behavior with two-step dehydrazination followed by one-step oxidative decarboxylation resulting into nanosize $Ni_{0.5-x}Mn_xZn_{0.5}Fe_2(C_4H_2O_4)_3.6N_2H_4$ ($x = 0.0–0.5$).
4. All the synthesized complexes display self propagating autocatalytic behavior once ignited, hence they can serve as single source precursor for synthesis of nanocrystalline mixed metal oxides at considerably lower temperatures.
5. The XRD studies of decomposed end products indicate the formation of the monophasic $Ni_{0.5-x}Mn_xZn_{0.5}Fe_2O_4$ ($x = 0.0–0.5$) ferrites. The FTIR spectral studies also support the results.
6. The broadening observed for XRD peaks suggests the nanocrystalline nature of mixed $Ni_{0.5-x}Mn_xZn_{0.5}Fe_2O_4$ ($x = 0.0–0.5$) ferrites. The average particle size obtained using Scherrer formula is in the range of 19–28 nm.
7. The TEM studies confirmed the nanosize nature of $Ni_{0.5-x}Mn_xZn_{0.5}Fe_2O_4$ ($x = 0.0–0.5$) ferrites with particle size in the range of 12–50 nm.

Acknowledgements

Authors are grateful for the financial support from DST, New Delhi through the Nano Mission project, No. SR/NM/NS-86/2009 and also under FIST. The authors are also thankful to UGC, New Delhi for the financial support under SAP and minor research project. The authors would like to acknowledge SAIF-IIT Bombay and Mr. Girish Prabhu, N.I.O., Goa for recording TEM and XRD of the samples, respectively.

References

[1] C. Caizer, M. Propovici, C. Savii, Spherical $(Zn_\delta Ni_{1-\delta}Fe_2O_4)_\gamma$ nanoparticles in an amorphous $(SiO_2)_{1-\gamma}$ matrix, prepared with the sol-gel method, Acta Mater. 51 (2003) 3607–3616.
[2] C.F.M. Costa, A.M.D. Leite, H.S. Ferreira, R.H.G.A. Kiminami, S. Cava, L. Gama, Brown pigment of the nanopowder spinel ferrite prepared by combustion reaction, J. Eur. Ceram. Soc. 28 (2008) 2033–2037.
[3] A. Goldman, Modern Ferrite Technology, 2nd ed., John Wiley, New York, 1990, p. 145.
[4] C. Venkatraju, G. Sathishkumar, K. Sivakumar, Effect of cation distribution on the structural and magnetic properties of nickel substituted nanosized Mn–Zn ferrites prepared by co-precipitation method, J. Magn. Magn. Mater. 322 (2010) 230–233.
[5] S.S. Jadhav, S.E. Shirsath, B.G. Toksha, S.J. Shukla, K.M. Jadhav, Effect of cation proportion on the structural and magnetic properties of Ni-Zn Ferrites nanosize particles prepared by co-precipitation technique, Chin. J. Chem. Phys. 21 (4) (2008) 381–386.
[6] A. Verma, R. Chatterjee, Effect of zinc concentration on the structural, electrical and magnetic properties of mixed Mn–Zn and Ni–Zn ferrites synthesized by citrate precursor technique, J. Magn. Magn. Mater. 306 (2006) 313–320.
[7] A.K. Singh, T.C. Goel, R.G. Mendiratta, Effect of cation distribution on the properties of $Mn_{0.2}Zn_xNi_{0.8-x}Fe_2O_4$, Solid State Commun. 12 (2003) 121–125.
[8] A.R. Bueno, M.L. Gregori, M.C.S. Nobrega, Microwave absorbing properties of $Ni_{0.5-x}Zn_{0.5-x}Me_{2x}Fe_2O_4$ (Me=Cu, Mn, Mg) ferrite-wax composite in X-band frequencies, J. Magn. Magn. Mater. 320 (2008) 864–870.
[9] M. Stefanescu, M. Stoia, O. Stefanescu, P. Barvinshi, Obtaining of $Ni_{0.65}Zn_{0.35}Fe_2O_4$ nanoparticles at low temperature starting from metallic nitrates and polyols, J. Therm. Anal. Calorim. 99 (2) (2010) 459–464.
[10] N. Deb, Thermal decomposition of manganese (II) bis(oxalato) nickelate(II) tetrahydrate, J. Therm. Anal. Calorim. 81 (2005) 61–65.
[11] O. Carp, L. Patron, G. Pascu, L. Mindru, N. Stanica, Thermal investigations of nickel–zinc ferrites formation from malate coordination compounds, J. Therm. Anal. Calorim. 84 (2) (2006) 391–394.

[12] R.K. Kamat, G.M. Naik, V.M.S. Verenkar, Synthesis and characterization of nickel manganite from different carboxylate precursors for thermistor sensors, Analog Applications (February) (2001) 52–56.
[13] D.N. Bhosale, V.M.S. Verenkar, K.S. Rane, P.P. Bakare, S.R. Sawant, Initial Susceptibility studies on Cu–Mg–Zn ferrites, Mater. Chem. Phys. 59 (1) (1999) 57–62.
[14] K.C. Patil, D. Gajapathy, V.R. Pai Vernekar, Low temperature cobaltite formation using mixed metal oxalate hydrazinate precursor, J. Mater. Sci. Lett. 2 (1983) 272–274.
[15] K.S. Rane, V.M.S. Verenkar, Synthesis of ferrite grade γ-Fe_2O_3, Bull. Mater. Sci. 24 (2001) 39–45.
[16] A. More, V.M. S. Verenkar, Synthesis of ultrafine nickel ferrite by autocatalytic decomposition of a novel precursor at room temperature, in: Dhirendra Bahadur, Satish Vitta, Om praksh (Eds.), Inorganic Materials: Recent Advances, Narosa Publishing House, New Delhi, 2004, pp. 23–32.
[17] D. Gajapathy, K.C. Patil, Mixed metal oxalate hydrazinates as compound precursors to spinel ferrites, Mater. Chem. Phys. 9 (1983) 423–438.
[18] V.M.S. Verenkar, R.A. Porob, S.Y. Sawant, K.R. Kannan, Synthesis, characterisation and thermal analysis of nickel manganese succinato hydrazinate, in: K.D. Mudher Singh, S. Bharadwaj, P.V Ravindran, S.K. Sali, V. Venugopal (Eds.), Proceedings of the 14th National Symposium on Thermal Analysis, Thermans 2004, Indian Thermal Analysis Society, Vadodara, India, 2004, pp. 335–337.
[19] R.A. Porob, S.Z. Khan, S.C. Mojumdar, V.M.S. Verenkar, T.G. Synthesis, DSC and spectral study of $NiMn_2(C_4H_4O_4)_3{\cdot}6N_2H_4$ A precursor for $NiMn_2O_4$ nanoparticles, J. Therm. Anal. Calorim. 86 (3) (2006) 605–608.
[20] B.N. Sivasankar, S. Govindarajan, Hydrazine mixed metal malonates – new precursors for metal cobaltites, Mater. Res. Bull. 31 (1) (1996) 47–54.
[21] K.S. Rane, H. Uskaikar, R. Pednekar, R. Mhalsikar, The low temperature synthesis of metal oxides by novel hydrazine method, J. Therm. Anal. Calorim. 90 (3) (2007) 627–638.
[22] M.M.A. Sekar, K.C. Patil, Hydrazine carboxylate precursors to fine titania, zirconia and zirconium titanate, Mater, Res. Bull. 28 (1983) 485–492.
[23] P. Ravindranathan, K.C. Patil, Thermal reactivity of metal formate hydrazinates, Thermochim. Acta 71 (1983) 53–57.
[24] G.V. Mahesh, K.C. Patil, Thermal reactivity of metal acetate hydrazinates, Thermochim. Acta 99 (1) (1986) 153–158.
[25] D. Gajapathy, K.C. Patil, V.R. Pai Vernekar, Low temperature ferrite formation using metal oxalate hydrazinate precursor, Mater. Res. Bull. 17 (1) (1982) 29–32.
[26] D. Gajapathy, K.C. Patil, K. Kishore, Thermal reactivity of metal oxalate hydrazinates, Thermochim. Acta 52 (1982) 113–120.
[27] B.N. Sivasankar, S. Govindarajan, Studies on *bis*(hydrazine) metal malonates and succinates, Synth. React. Inorg. Met. Org. Chem. 24 (9) (1994) 1573–1582.
[28] B.N. Sivasankar, Cobalt(II), nickel(II) and zinc(II) dicarboxylate complexes with hydrazine as bridged ligand: Characterization and thermal degradation, J. Therm. Anal. Calorim. 86 (2) (2006) 385–392.
[29] B.N. Sivasankar, S. Govindrajan, Acetate and malonate complexes of cobalt (II), nickel(II) and zinc(II) with hydrazinium cation: Preparation, spectral and thermal studies, J. Therm. Anal. 48 (6) (1997) 1401–1413.
[30] S. Govindrajan, S.U.N. Banu, N. Sarayanan, B.N. Sivasankar, *Bis*-hydrazine metal maleates and fumarates: preparation, spectral and thermal studies, Proc. Ind. Acad. Sci. (Chem. Sci.) 107 (5) (1995) 559–565.
[31] V.M.S. Verenkar, K.S. Rane, Synthesis, characterisation and thermal analysis of ferrous malato-hydrazinate, in: P.V. Ravindran, M. Sudersanan, N.L. Misra, V. Venugopal (Eds.), Proceedings of the 12th National Symposium on Thermal Analysis, Thermans 2000, Indian Thermal Analysis Society, Gorakhpur, India, 2000, pp. 194–195.
[32] V.M.S. Verenkar, R.A. Porob, S.Y. Sawant, K.R. Kannan, Synthesis, characterisation and thermal analysis of nickel manganese fumarato-hydrazinate, in: C.G.S. Pillai, K.L. Ramakumar, P.V. Ravindran, V. Venugopal (Eds.), Proceedings of the 13th National Symposium on Thermal Analysis, Thermans 2002, Indian Thermal Analysis Society, Mumbai, India, 2002, pp. 154–155.
[33] S.Y. Sawant, V.M.S. Verenkar, S.C. Mojumdar, Preparation, thermal XRD, chemical and FTIR spectral analysis of $NiMn_2O_4$ nanoparticles and respective precursor, J. Therm. Anal. Calorim. 90 (3) (2007) 669–672.
[34] A. More, V.M.S. Verenkar, S.C. Mojumdar, Nickel ferrite nanoparticles synthesis from novel fumarato-hydrazinate precursor, J. Therm. Anal. Calorim. 94 (1) (2008) 63–67.
[35] U.B. Gawas, S.C. Mojumdar, V.M.S. Verenkar, $Ni_{0.5}Mn_{0.1}Zn_{0.4}Fe_2(C_4H_2O_4)_3{\cdot}6N_2H_4$ precursor, $Ni_{0.5}Mn_{0.1}Zn_{0.4}Fe_2O_4$ nanoparticles: preparation, IR spectral, XRD, SEM-EDS and thermal analysis, J. Therm. Anal. Calorim. 96 (1) (2009) 49–52.
[36] L.R. Gonsalves, V.M.S. Verenkar, S.C. Mojumdar, Preparation and characterization of $Co_{0.5}Zn_{0.5}Fe_2(C_4H_2O_4)_3{\cdot}6N_2H_4$: a precursor to prepare $Co_{0.5}Zn_{0.5}Fe_2O_4$ nanoparticles, J. Therm. Anal. Calorim. 96 (1) (2009) 53–57.
[37] U.B. Gawas, S.C. Mojumdar, V.M.S. Verenkar, Synthesis, characterization infrared studies, and thermal analysis of $Mn_{0.6}Zn_{0.4}Fe_2(C_4H_2O_4)_3{\cdot}6N_2H_4$ and its decomposition product $Mn_{0.6}Zn_{0.4}Fe_2O_4$, J. Therm. Anal. Calorim. 100 (3) (2010) 867–871.
[38] L.R. Gonsalves, S.C. Mojumdar, V.M.S. Verenkar, Synthesis of cobalt nickel ferrite nanoparticles via autocatalytic decomposition of the precursor, J. Therm. Anal. Calorim. 100 (3) (2010) 789–792.
[39] L.R. Gonsalves, S.C. Mojumdar, V.M.S. Verenkar, Synthesis and characterization of $Co_{0.8}Zn_{0.2}Fe_2O_4$ nanoparticles, J. Therm. Anal. Calorim. 104 (3) (2011) 869–873.
[40] U.B. Gawas, V.M.S. Verenkar, S.C. Mojumdar, Synthesis and characterization of $Ni_{0.6}Zn_{0.4}Fe_2O_4$ nano-particles obtained by auto catalytic thermal decomposition of carboxylato-hydrazinate complex, J. Therm. Anal. Calorim. 104 (3) (2011) 879–883.
[41] L.R. Gonsalves, S.C. Mojumdar, V.M.S. Verenkar, Synthesis and characterization of ultrafine spinel ferrites obtained by precursor combustion technique, J. Therm. Anal. Calorim. 108 (3) (2012) 859–863.
[42] U.B. Gawas, V.M.S. Verenkar, S.C. Mojumdar, Nano-crystalline $Mn_{0.3}Ni_{0.3}Zn_{0.4}Fe_2O_4$ obtained by novel fumarato-hydrazinate precursor method: synthesis, characterization and studies of magnetic and electrical properties, J, Therm. Anal. Calorim. 108 (3) (2012) 865–870.
[43] L.R. Gonsalves, V.M.S. Verenkar, Synthesis and thermal studies of the cobalt zinc ferrous fumarato-hydrazinate: a precursor to obtained nanosize ferrites, J. Therm. Anal. Calorim. 108 (3) (2012) 871–875.
[44] L.R. Gonsalves, V.M.S. Verenkar, Synthesis and characterization of nanosize nickel doped cobalt ferrite obtained by precursor combustion technique, J. Therm. Anal. Calorim. 108 (3) (2012) 877–880.
[45] Vogel's Text book of Quantitative Inorganic Analysis (Revised by G.H. Jeffery, J. Bassett, J. Mendham and R.C. Denney), fifth ed., Longman, UK, 1989, pp. 334, 402, 457, 462.
[46] P. Pramanik, A. Pathak, A new chemical route for the preparation of fine ferrite powders, Bull. Mater. Sci. 17 (1994) 967–976.
[47] P.P. Sarangi, B.D. Naik, N.N. Ghosh, Synthesis of single-phase α-Fe_2O_3 nanopowders by using a novel low temperature chemical synthesis route, J. Am. Ceram. Soc. 91 (2008) 4145–4147.
[48] A. Braibanti, F. Dallavalle, M.A. Pellinghelli, E. Leporati, The nitrogen–nitrogen stretching band in hydrazine derivatives and complexes, Inorg. Chem. 7 (1968) 1430–1433.
[49] R. Tsuchiya, M. Yonemura, A. Uehera, E. Kyuno, Derivatographic studies on transition metal complexes. XIII. Thermal decomposition of $[Ni(N_2H_4)_6]X_2$ complexes, Bull. Chem. Soc. Jpn. 47 (3) (1974) 660–664.
[50] K. Nakamoto, Infrared Raman Spectra of Inorganic and Coordination Compounds Part B, 6th ed., John Wiley, New York, 1978, 153.
[51] R.D. Waldron, Infrared spectra of ferrites, Phys. Rev. 99 (1955) 1727–1735.
[52] T.T. Srinivasan, C.M. Srivastava, N. Venkataramani, M.J. Patni, Infrared absorption in spinel ferrites, Bull. Mater. Sci. 6 (6) (1984) 1063–1067.